IJPSR (2019), Volume 10, Issue 4 (Research Article)

INTERNATIONAL JOURNAL OF PHARMACEUTICAL SCIENCES AND RESEARCH

Received on 17 July 2018; received in revised form, 28 September 2018; accepted, 05 October 2018; published 01 April 2019

NANOEMULSION FOR IMPROVED PERMEABILITY OF *CENTELLA ASIATICA* EXTRACT: FORMULATION, *EX-VIVO* AND *IN-VIVO* EVALUATION

R. R. Lala * and P. H. Patel

Prin. K. M. Kundnani College of Pharmacy, Cuffe Parade, Mumbai - 400005, Maharashtra, India.

Keywords:

Centella asiatica extract, Photoaging, Nanoemulsion, Pseudoternary phase diagram

Correspondence to Author:
Dr. Rita R. Lala

Assistant Professor,
Department of Pharmaceutics,
Prin. K. M. Kundnani College of Pharmacy, Cuffe Parade, Mumbai - 400005, Maharashtra, India.

E-mail: r_r_lala@yahoo.co.in

ABSTRACT: *Centella asiatica* L. Urban (family: Umbelliferae) contains several active triterpenoids which have been reported to induce type I collagen which decreases substantially in photoaged skin. *Centella asiatica* extract is highly soluble in water but have low absorption into the skin. To overcome this, water in oil nanoemulsion loaded with *Centella asiatica* extract have been formulated, optimized and evaluated as the potential delivery system for treating photoaging. Nanoemulsions were formulated by the oil phase titration method and optimized by constructing pseudo-ternary phase diagrams. The prepared nanoemulsions were subjected to thermodynamic stability testing. Those that passed these tests were characterized for droplet size, polydispersity index, zeta potential and droplet morphology by Cryo-SEM. The prepared nanoemulsions were in nanometric range (optimized batch: 140.5 nm) with uniform size distribution (PDI: 0.086) and good physical stability (zeta potential: -33.9 mV). Topical permeation of *Centella asiatica* loaded nanoemulsion through porcine abdominal skin was estimated using the Franz diffusion cell. A significant increase in permeability parameters was observed in nanoemulsion formulations (P<0.05) as compared to an aqueous solution of *Centella asiatica* extract. Topical application of CA nanoemulsion loaded cream to rat hind limb significantly reduced the wrinkle formation on UV exposed skin. Histopathological studies of the skin samples further confirmed the antiphotoaging effects of the prepared nano-emulsion formulation.

INTRODUCTION: Skin aging is a natural phenomenon. But many times premature aging of the skin occurs due to external factors which lead to photoaging of skin. 'Photoaging' is the process by which sunlight or artificial ultraviolet radiation (UV) gradually induces clinical and histological changes in the skin. Cosmeceuticals are achieving increased popularity in the personal care industry. The significant share of this growing cosmeceutical industry comes from the age-defying products.

QUICK RESPONSE CODE

DOI: 10.13040/IJPSR.0975-8232.10(4).1711-18

The article can be accessed online on www.ijpsr.com

DOI link: http://dx.doi.org/10.13040/IJPSR.0975-8232.10(4).1711-18

Several synthetic skincare cosmeceuticals are existing in the market to treat photoaging, and the most common adverse reactions of those include allergic contact dermatitis, irritant contact dermatitis, phototoxic and photoallergic reactions. Therefore, the use of natural and herbal based products has become a new trend. *Centella asiatica* L. Urban (family: Umbelliferae) is a perennial herb containing several active triterpenoids, saponins, including madecassoside, asiaticoside, centelloside and asiatic acid which has been reported to induce type I collagen which decreases substantially in photoaged skin [1].

Nanoemulsions are thermodynamically stable transparent or translucent dispersions of water and oil stabilized by an interfacial film of surfactant usually in combination with co-surfactant having

droplet size between 20-600 nm [2]. Nanoemulsions are a promising technique for transdermal delivery of herbal extracts and offer various advantages like improved penetration, low irritation, higher storage stability and controlled delivery of active principles. *Centella asiatica* extract is highly soluble in water but have low absorption into the skin. This is because the active triterpenoids have high molecular size and are thus unable to cross the lipid membrane of the cells [3].

The aim of this work reported herein was to formulate a nanoemulsion system by construction of ternary phase diagram using *Centella asiatica* extract in the aqueous phase, natural oils (Grapeseed, Walnut, and Wheatgerm) as oil phase stabilized by span 80 and labrasol.

MATERIALS AND METHODS: *Centella asiatica* extract was received as a gift sample from Pharmanza Herbals (Gujarat). Propylene glycol monocaprylate (Capryol 90), propylene glycol dicaprylocaprate (Labrafac), oleoyl polyoxyl-6 glycerides (Labrafil), glyceryl monolinoleate (Maisine), diethylene glycol monoethyl ether (Transcutol P) were kind gift samples from Gattefossé (France). Wheatgerm oil, grapeseed oil, and walnut oil were obtained from Aromex Industries (Mumbai). Polyoxyethylene 80 sorbitan monooleate, sorbitan oleates, cocoa butter were obtained from S.D Fine (Mumbai). All other chemicals used in the study were of analytical reagent (AR) grade.

Screening of Oils and Surfactants: The solubility of *Centella asiatica* extract in various oils, surfactants and distilled water were determined by dissolving an excess amount of *Centella asiatica* extract in 2 ml of each of the selected oils and surfactants and were mixed for 10 min using a vortex mixture. The vials were then kept at 37 ± 1.0°C for 72 h to equilibrate. The equilibrated samples were centrifuged at 3,000 rpm for 15 min. The supernatant was filtered, and the concentration of *Centella asiatica* extract was determined in each oil and surfactant by UV spectrophotometer at the wavelength of 225 nm.

Determination of Optimum Surfactant and Cosurfactant: [4, 5] At a fixed S_{mix} ratio of 1:1, the pseudoternary phase diagrams were constructed by oil phase titration method. Nine different combinations in different weight ratios of water and S_{mix}, 1:9, 2:8, 3:7, 4:6, 5:5, 6:4, 7:3, 8:2 and 9:1 were taken so that maximum ratios were covered to delineate the boundaries of phases precisely formed in the phase diagrams. The nanoemulsion phase was identified as the region in the phase diagram where clear, readily flowable, and transparent formulations were obtained based on the visual observation.

Effect of Surfactant and Cosurfactant Mass Ratio on Nanoemulsion Formation: [6] Surfactant (Span 80) was blended with cosurfactant (Labrasol) in the weight ratios of 3:1, 2:1, 1:1, 1:0, 1:2, and 1:3. These S_{mix} ratios were chosen in decreasing concentration of surfactant concerning the cosurfactant and increasing concentration of cosurfactant concerning surfactant for a detailed study of the phase diagrams. Nine different combinations in different weight ratios of water and S_{mix}, 1:9, 2:8, 3:7, 4:6, 5:5, 6:4, 7:3, 8:2 and 9:1 were taken.

Preparation of *Centella asiatica* Extract Containing Nanoemulsion Formulations: From each phase diagram constructed, different formulae were selected from nanoemulsion region for the incorporation of the *Centella asiatica* extract into the aqueous phase. 1% *Centella asiatica* extract was dissolved in the aqueous phase, and the oil phase was added slowly with continuous stirring. The emulsion obtained was further homogenized at high speed to achieve transparent water in oil nano-emulsions with uniform size distribution.

Dispersion Stability Tests: [4] To evaluate the physical stability of the formulations, thermodynamic stability tests were performed. Selected formulations were subjected to different thermodynamic stability tests to overcome the problem of metastable formulations.

Heating-Cooling Cycle: Six cycles between refrigerator temperature (4 °C) and 45 °C with storage at each temperature of not less than 48 h were carried out, and the formulations were examined for stability at these temperatures.

Centrifugation Test: Formulations were centrifuged at 3,500 rpm for 30 min, and observed for phase separation, creaming or cracking.

Freeze-Thaw Cycle: This test evaluated the accelerated stability of nanoemulsion formulations. Three freeze-thaw cycles between -21 °C and +25°C, with formulation storage at each temperature for not less than 48 h, were performed.

The formulations which showed no phase separation, creaming, coalescence or phase inversion upon these tests were selected for characterization.

Incorporation of Optimized Nanoemulsion into a Base: The optimized nanoemulsion was incorporated into a base consisting of Shea butter, cocoa butter, and hard paraffin to obtain the final formulation in the form of a cream.

Droplet Size and Polydispersity Index: [5] Droplet size and polydispersity index (PDI) were measured by a Malvern Zetasizer Nano ZS (Malvern Instrument Ltd., UK) at a fixed angle of 173° at 25 °C. Before the measurements, all samples were diluted with liquid paraffin to produce a suitable scattering intensity.

Zeta Potential Analysis: [7, 8] Zeta potential measurements were performed using Nano sight NS 500 (Malvern Instruments Ltd, UK) which measures the electrophoretic mobility of the particles in an electrical field.

Morphology of Droplets: [9] Cryogenic field emission gun scanning electron microscopy (Cryo-FEG SEM) was performed to visualize droplet morphology. Approximately 10 µl of nanoemulsion sample was deposited on a carbon tape and frozen in liquid nitrogen. Samples were then immediately transferred into the cryo-preparation chamber and freeze-fractured on the cryo-stage. The sample was then sputter coated with platinum for 60 sec in the cryo-preparation chamber. The sample was then inserted into the field emission gun scanning electron microscope (JSM-7600F) examined at an accelerating voltage of 5.0 kV.

***Ex-vivo* Permeability Study:** [11, 14] *Ex-vivo* skin permeation studies were performed using porcine abdominal skin with a Franz diffusion cell having an effective diffusion area of 5.726 cm^2 and 18 ml receiver chamber capacity. Full-thickness porcine skin was excised from the abdominal region and hair was removed with an electric clipper. The subcutaneous tissue was removed surgically, and the dermis side was wiped with isopropyl alcohol to remove adhering fat. The skin was mounted between the donor and receiver compartments of the Franz diffusion cell, with the stratum corneum side facing the donor compartment and the dermal side facing the receiver compartment. The receiver chamber was filled with phosphate-buffered saline (PBS) solution pH 7.4, stirred with a magnetic rotor at a speed of 100 rpm, and maintained at a temperature of 32 ± 1 °C. Two ml of the optimized nanoemulsion formulation (equivalent to 2 mg/mL CA extract) was placed in the donor compartment and sealed with aluminum foil to provide occlusive conditions. Samples were withdrawn at regular intervals (0.5, 1, 2, 3, 4, 5, 6, 7 and 8 h) and sink conditions were maintained by replacement with fresh medium. Samples were filtered and analyzed for drug content by UV spectro-photometer. All the experiments were performed in triplicates.

Permeation Data Analysis: The cumulative amount of drug permeated through the skin (µg/cm^2) was plotted as a function of time (t) for each formulation. Drug flux (permeation rate) at steady state (J_{ss}) was calculated by dividing the slope of the linear portion of the graph by the area of the diffusion cell. The permeability coefficient (K_p) was calculated by dividing Jss by the initial concentration of drug in the donor cell (C_o):

$$K_p = J_{ss} / C_o$$

Enhancement ratio (E_r) was calculated by dividing the J_{ss} of the respective formulation by the J_{ss} of the control formulation:

$$E_r = J_{ss} \text{ of formulation} / J_{ss} \text{ of control}$$

***In-vivo* Studies:**

Study of Anti-Wrinkle Activity: [12] The *in-vivo* studies were initiated after obtaining approval from the Institutional Animal Ethics Committee (protocol no: KMKCP/IAEC/161707). The Wistar rats were placed in cages individually, and their hind limb skin was irradiated using a UV lamp without any filtering for 6 weeks. The distance from the lamp to the animal's hind limb was 42 cm. A dose of UV radiation was given three times weekly for five minutes.

Animals were randomly divided into three groups of six rats each: Group 1-control group not exposed to UV light or treated topically with any material, Group 2 - animals exposed to UV light followed by blank formulation and Group 3 - animals exposed to UV light followed by topical application of prepared nanoformulation. Sample (test and blank respectively) were applied to each unilateral hind limb skin of rats at the same time each day, five times a week for 6 weeks. On the days when rats were UV radiated, samples were applied immediately after the UV radiation. The hind limb skin of rats will be assessed as the following table.

TABLE 1: WRINKLE SCORING

Grade	Wrinkle
0	No coarse wrinkle
1	A few shallow, coarse wrinkles
2	Some coarse wrinkle
3	Several deep wrinkles

Histopathological Evaluation: The skin specimens including full-thickness skin layers (epidermis, dermis, and hypodermis) were fixed in 10% buffered formaldehyde and processed according to routine light microscope tissue processing method. Processed tissues were embedded in paraffin, and tissue sections stained with haematoxylin and eosin (H&E stain) and Van Gieson's stain were examined.

RESULTS AND DISCUSSION

Screening of Oils and Surfactants: The solubility of *Centella asiatica* extract was found to be maximum in capryol 90 (24.85 ± 0.20 mg/mL) compared to other oils. Thus, capryol 90 was selected as the main component of the oil phase. Since wheat germ oil, grape seed oil, and walnut oil have cosmeceutical application, they are also incorporated in the oil phase. The final oil phase consists of capryol 90 (50%), wheat germ oil (30%), walnut oil (15%) and grape seed oil (5%).

Since the solubility of *Centella asiatica* extract is found to be higher in distilled water (60.90 ±1.07 mg/mL) than in oils, w/o nanoemulsions as a potential delivery system are investigated. Based on solubility, span 80 and tween 80 were selected as surfactants and labrafil and labrasol were selected as the co-surfactants.

Determination of Optimum Surfactant and Cosurfactant: Nanoemulsion area was used as the parameter for determining the optimum combination of surfactant and cosurfactant. The nanoemulsion region in the phase diagrams was compared at the fixed S_{mix} ratio of 1:1. It was observed that batch 4 consisting of span 80 and labrasol had the maximum nanoemulsion area followed by batch 3 consisting of span 80 and labrafil. This can be attributed to the fact that water in oil nanoemulsions requires a surfactant with low HLB value for its stable formation. The maximum area of a nanoemulsion of batch 4 must be due to the optimum value of HLB (9.15) of the mixture of surfactant and co-surfactant which is required for the formation of water in oil nanoemulsions. It was observed that as the HLB value of the mixture increased above 11 the nanoemulsion area for water in oil nanoemulsion decreased.

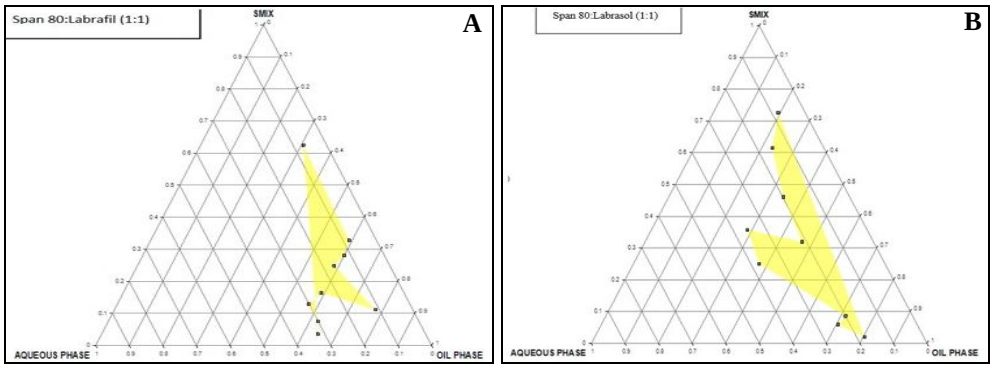

FIG. 1: PSEUDOTERNARY PHASE DIAGRAMS OF A) SPAN 80: LABRAFIL (1:1) B) SPAN 80: LABRASOL (1:1)

Effect of Surfactant and Cosurfactant Mass Ratio on Nanoemulsion Formation: A low-nanoemulsion area was observed when span 80 was used alone without cosurfactant, *i.e.*, at the S_{mix} ratio 1:0. This must be because Span 80 being lipophilic, it is not able to sufficiently reduce the

water-oil interfacial tension in the absence of a cosurfactant. When cosurfactant was added with surfactant in equal amounts, a higher nanoemulsion region was observed, perhaps because of the further reduction of the interfacial tension and increased fluidity of the interface at S_{mix} 1:1. When the surfactant concentration is further increased in the S_{mix} ratio of 3:1, a decrease in the nanoemulsion region was observed when compared with S_{mix} 2:1.

It can be said that, when surfactant concentration was increased in comparison to cosurfactant, the nanoemulsion region increased up to the 2:1 S_{mix} ratio, but in the 3:1 ratio, it was decreased, indicating that the optimum emulsification has been achieved. When the cosurfactant concentration concerning surfactant was increased to the S_{mix} 1:2, it was observed that the nanoemulsion area decreased as compared to S_{mix} 1:1. This indicates that although the cosurfactant contributes to the interfacial properties, at higher concentration, it alters the emulsification of surfactant and causes a decrease in aqueous phase solubilization.

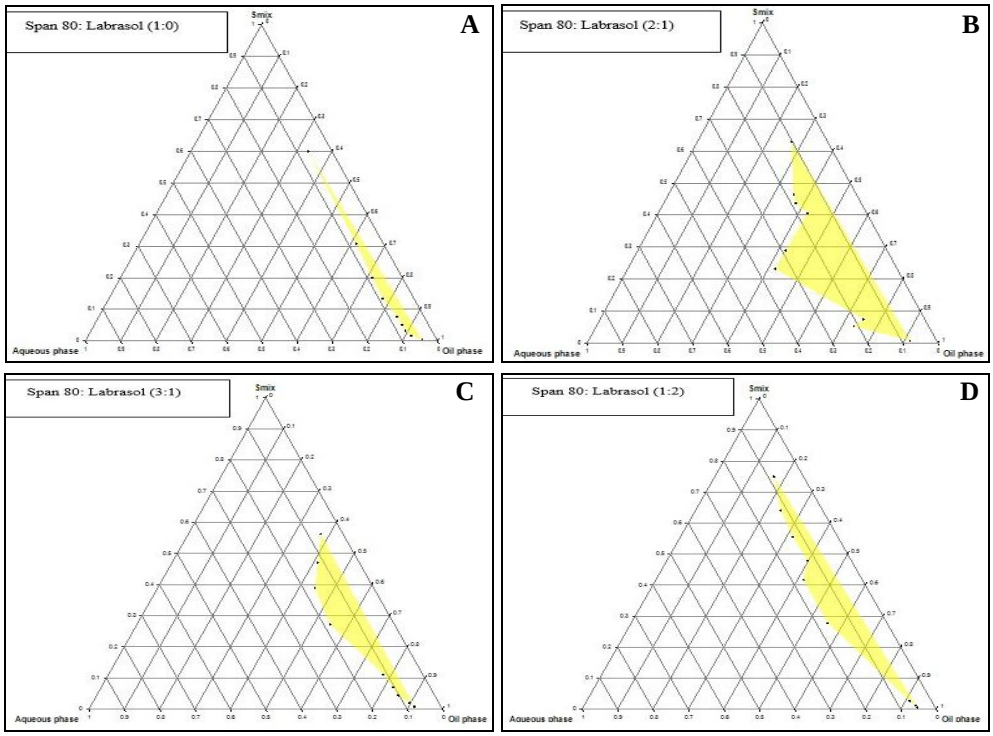

FIG. 2: PSEUDO TERNARY PHASE DIAGRAMS OF A) SPAN 80: LABRASOL (1:0) B) SPAN 80: LABRASOL (2:1) C) SPAN 80: LABRASOL (3:1) D) SPAN 80: LABRASOL (1:2)

Preparation of Nanoemulsion Formulation: From the phase diagrams, different formulae from nanoemulsion region were selected for incorporation of the *Centella asiatica* extract into the aqueous phase.

TABLE 2: COMPOSITION OF DIFFERENT BATCHES FROM PHASE DIAGRAMS

S_{mix} ratio	Code	Percentage of different components in the formulation		
		Aqueous phase	S_{mix}	Oil phase
3:1	A1	25	30	45
	A2	20	25	55
	A3	15	25	60
	A4	10	20	70
1:1	B1	35	28	37
	B2	35	30	35
	B3	31	28	41
	B4	17	25	58
2:1	C1	15	30	55
	C2	20	40	40
	C3	25	35	45
	C4	30	40	30

Droplet Size and Polydispersity Index: The mean droplet size of *Centella asiatica* loaded nanoemulsions was found in the range of 140.5–248.70 nm. The polydispersity index was in the range 0.086 - 0.481 which indicates that all the formulations have uniform droplet size. Formulation C2 containing 20% aqueous phase and 40% oil phase showed least droplet size (140.5 nm) and lowest polydispersity index (0.086).

Zeta Potential: A stable dispersion might be formed when the values of zeta potential are above ± 30 mV. This is due to the presence of repulsion forces between particles that prevents them from aggregation. The zeta potential of all the nanoemulsion formulations was found to be in the range of -33.9 mV to -21.75 mV indicating stability of nanoemulsion formulations. The zeta potential of the optimized batch was found to be -33.9 mV.

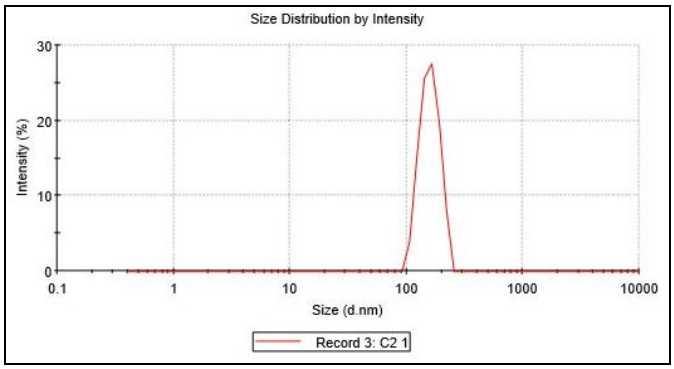

FIG. 3: DROPLET SIZE DISTRIBUTION OF OPTIMIZED BATCH

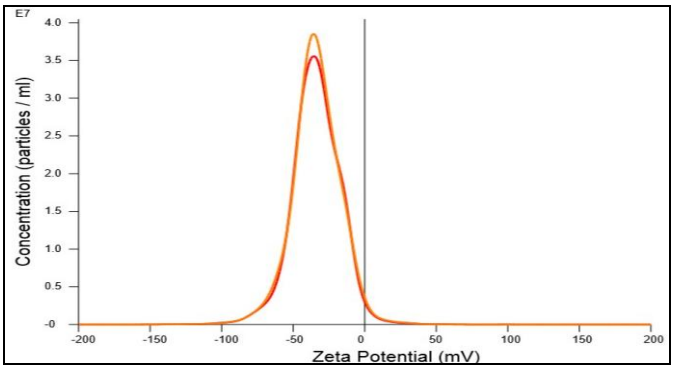

FIG. 4: ZETA POTENTIAL OF OPTIMIZED BATCH

Morphology of Droplets: In the cryo-FEG SEM micrographs, the droplets were highly uniform with an average droplet diameter smaller than 150 nm. These diameters of droplet observed in cryo-FEG SEM are in good accordance with the diameter values measured by dynamic light scattering.

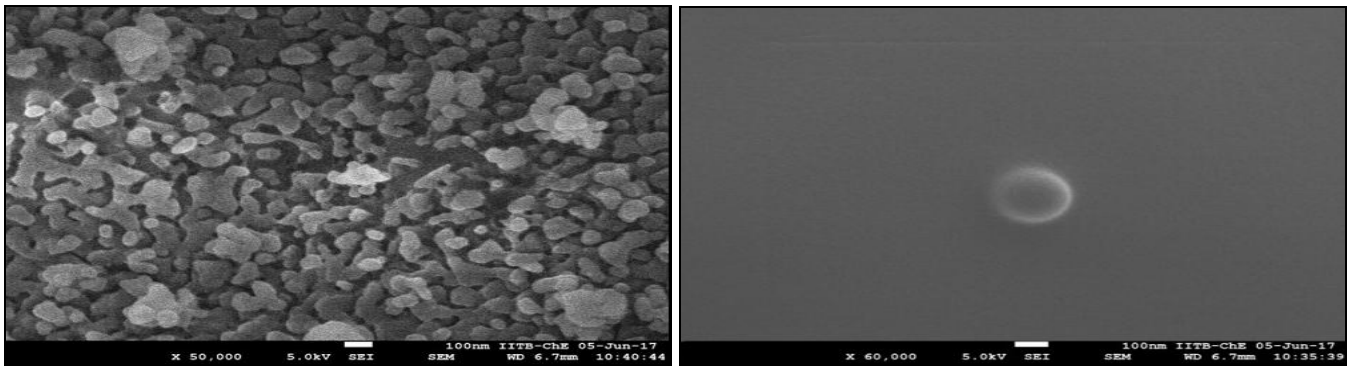

FIG. 5: CRYO-FEG SEM OF OPTIMIZED FORMULATION

***Ex-vivo* Skin Permeation:** The % cumulative release from porcine skin was found to be in the range of 61.77 to 85.15 %.

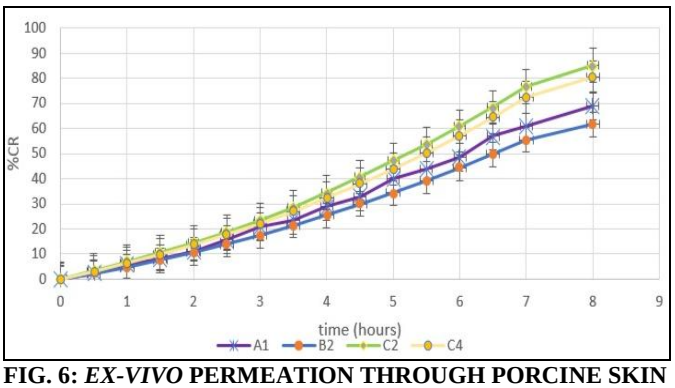

FIG. 6: *EX-VIVO* PERMEATION THROUGH PORCINE SKIN

The *ex-vivo* release of all the nanoemulsion formulations was significantly higher than the aqueous control (P<0.05). The highest *ex-vivo* release of formulation C2 as compared to other formulations can be attributed to the lowest droplet size. Also, the presence of capryol 90 and labrasol in the formulations lead to increased permeation as they act as permeation enhancers.

Anti Wrinkle Activity: The UV exposure induced heavy wrinkling in the rat skin. The degree of wrinkling was reduced by treatment with CA extract loaded nanoemulsion.

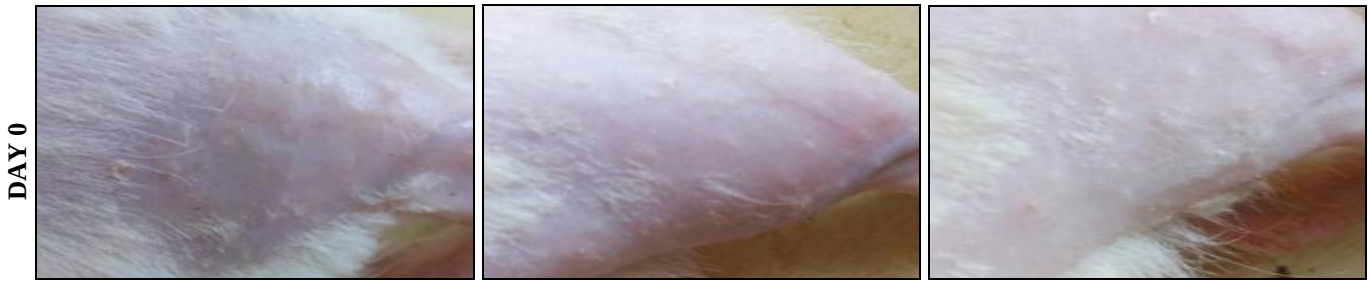

Group 1- Control **Group 2- UV + Blank Formulation** **Group 3- UV + Nanoformulation**

FIG. 7: RAT SKIN PHOTOGRAPHS AT DAY 0

Group 1- Control **Group 2- UV + Blank Formulation** **Group 3- UV + Nanoformulation**

FIG. 8: RAT SKIN CHANGES AT WEEK 6

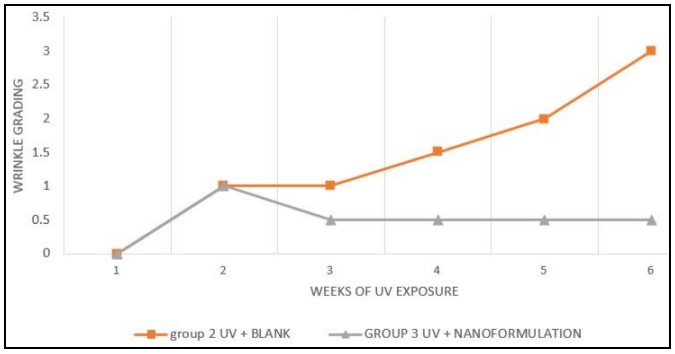

FIG. 9: SEQUENTIAL CHANGES IN WRINKLE SCORE WITH WEEKS. * $p < 0.05$ compared with corresponding UV + blank group (group 2).

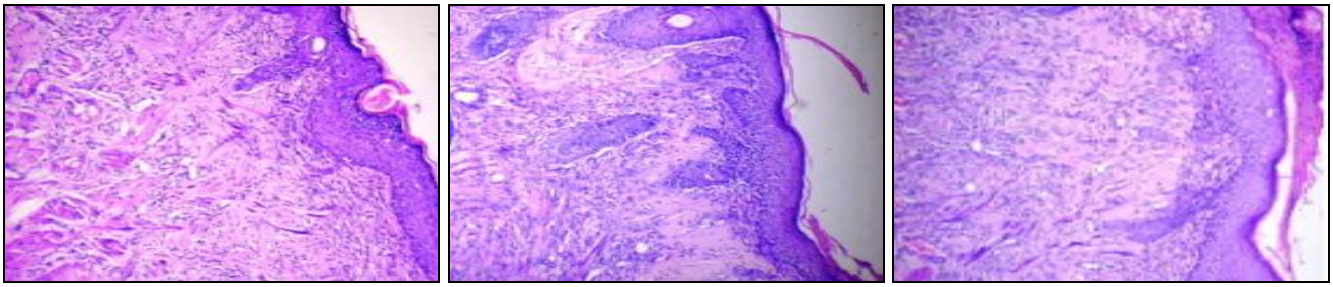

Group 1- Control **Group 2- UV + Blank Formulation** **Group 3- UV + Nanoformulation**

FIG. 10: H & E STAINING OF RAT SKIN

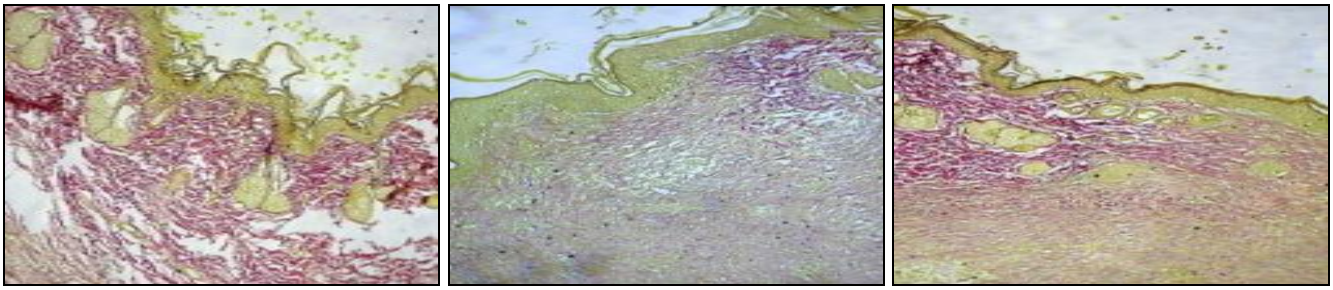

Group 1- Control **Group 2- UV + Blank Formulation** **Group 3- UV + Nanoformulation**

FIG. 11: VAN GIESON STAINING OF RAT SKIN

At treatment week 6, the mean wrinkle grade of the nanoformulation-treated group was 0.5, and that of the vehicle-treated group was 3, respectively. The difference in mean wrinkle grade between the two groups was significant.

Histopathological Evaluation: The hematoxylin and eosin (H & E) staining were performed to evaluate the epidermal epithelium. As seen in the microscopic observations the control group showed normal epidermal structure whereas mild and minimal degree hyperplasia was observed in vehicle-treated and formulation treated rat skin respectively. Van Gieson stain was used for collagen fibre staining. Group 2 *i.e*. vehicle-treated group showed moderate degree reduction in thickness of dermal collagen while formulation treated group showed no abnormalities in the dermal collagen thickness. This can be attributed to the fact that the active triterpenoids in the *Centella asiatica* extract are responsible for type 1 collagen synthesis.

CONCLUSION: In the present investigation, water in oil nanoemulsions loaded with *Centella asiatica* extract were successfully prepared by a phase titration method with capryol 90 along with wheat germ, walnut, and grapeseed oils as oil phase stabilized by span 80 and labrasol. The prepared nanoemulsions were in nanometric range (optimized batch: 140.5 nm) with uniform size distribution (PDI: 0.086) and good physical stability (zeta potential: -33.9 mV). Topical permeation of *Centella asiatica* loaded nano-emulsion through porcine abdominal skin was estimated using the Franz diffusion cell. A significant increase in permeability parameters was observed in nanoemulsion formulations ($P<0.05$) as compared to an aqueous solution of *Centella asiatica* extract. Topical application of CA nanoemulsion loaded cream to rat hind limb significantly reduced the wrinkle formation on UV exposed skin. Histopathological studies of the skin samples further confirmed the antiphotoaging effects of the prepared nanoemulsion formulation.

ACKNOWLEDGEMENT: The authors are thankful to Pharmanza Herbals for providing the gift sample of *Centella asiatica* extract and IIT-Bombay for providing Cryo-SEM facility.

CONFLICT OF INTEREST: The authors declare that they have no competing interests.

REFERENCES:

1. Bylka W, Znajdek-Awize P, Studziska-Sroka E and Brzeziska M: *Centella asiatica* in Cosmetology. Postep Dermatologii Alergol 2013; 30(1): 46-49.
2. Jaiswal M, Dudhe R and Sharma PK: Nanoemulsion: An advanced mode of drug delivery system. 3 Biotech 2015; 5(2): 123-127.
3. Bonifácio BV, da Silva PB, Aparecido dos Santos Ramos, M, Maria Silveira Negri K, Maria Bauab T and Chorilli M: Nanotechnology-based drug delivery systems and herbal medicines: A review. Int J of Nano-medicine 2014; 9(1): 1-5.
4. Mishra A and Saklani S: Formulation and evaluation of herbal antioxidant *Nardostachys jatamansi* collected from Indian Himalayan face cream of region. Asian Pac J Trop Biomed 2014; 4(2): 2-5.
5. Shakeel F and Ramadan W: Transdermal delivery of anticancer drug caffeine from water-in-oil nanoemulsions. Colloids Surfaces B Biointerfaces 2010; 75(1): 356-362.
6. Setya S, Negi P, Razdan BK and Talegaonkar S: Design, development and *in-vitro* investigation of water in oil nanoemulsion for transdermal delivery. World J Pharm Pharm Sci 2014; 3(12): 1495-1512.
7. Ostrosky EA, Rocha-filho PA and Veríssimo LM: Production and characterization of cosmetic nano-emulsions containing Opuntia *F. indica* (L.) Mill extract as a moisturizing agent. Molecules 2015; 1: 2492-2509.
8. Siddalingam R and Chidambaram K: Topical nano-delivery of 5-fluorouracil : Preparation and characterization of water-in-oil nanoemulsion. Trop J Pharm Res 2016; 15(11): 2311-19.
9. Klang V, Matsko NB, Valenta C and Hofer F: Electron microscopy of nanoemulsions: An essential tool for characterization and stability assessment. Micron 2012; 43(2-3): 85-103.
10. Tabibiazar M and Hamishehkar H: Formulation of a food grade water-in-oil nanoemulsion: Factors affecting on stability. Pharm Sci 2015; 21(4): 220-224.
11. Awari RRLNG: Nanoemulsion-based gel formulations of COX-2 Inhibitors for enhanced efficacy in inflammatory conditions. Appl Nanosci 2014; 4: 143-151.
12. Lee HJ, Kim JS, Song MS, Seo HS, Moon C, Kim JC, Jo SK, Jang JS and Kim SH: Photoprotective effect of red ginseng against ultraviolet radiation-induced chronic skin damage in the hairless mouse. Phyther Res 2009; 23(3): 399-403.
13. Chavda VP and Shah D: A review on novel emulsification technique : A Nanoemulsion. Journal of Pharmacology and Toxicological Studies 2017; 5(1): 29-37.
14. Jaiswal M, Kumar A and Sharma S: Nanoemulsions Loaded carbopol 934 based gel for intranasal delivery of neuroprotective *C. asiatica* extract: *In-vitro* and *Ex-vivo* permeation study. J Pharm Investig 2016; 46(1): 79-89.

How to cite this article:
Lala RR and Patel PH: Nanoemulsion for improved permeability of *Centella asiatica* extract: formulation, *ex-vivo* and *in-vivo* evaluation. Int J Pharm Sci & Res 2019; 10(4): 1711-18. doi: 10.13040/IJPSR.0975-8232.10(4).1711-18.